JURNAL INFOTEL
Informatics - Telecommunication - Electronics
Website: http://ejournal.st3telkom.ac.id/index.php/infotel
ISSN: 2085-3688; e-ISSN: 2460-0997

The combination of color-texture features and machine learning for detecting Dayak beads

Anindita Septiarini[1,*], Hamdani Hamdani[2], Edy Winarno[3]
[1,2]Department of Informatics, Faculty of Engineering, Mulawarman University
[3]Faculty of Information Technology & Industry, Universitas Stikubank
[1,2]Jl. Sambaliung, No. 9, Samarinda 75242, Indonesia
[3]Jl. Tri Lomba Juang, No. 1, Semarang 50241, Indonesia
[*]Corresponding email: anindita@unmul.ac.id

Received 19 November 2022, Revised 22 December 2022, Accepted 20 January 2023

Abstract — The Dayak are one of the indigenous people who reside in East Kalimantan, Indonesia. This region is home to a great deal of cultural diversity. One of the ancient crafts practiced by the Dayak is the creation of beads utilizing a variety of materials and distinct motifs. The Dayak beads include a wide variety of designs and color configurations that can be selected. Consequently, only some easily differentiate between the bead motif used by Dayak and non-Dayak. The purpose of this study aims to develop a bead detection method to differentiate between the bead types of Dayak and non-Dayak. The main processes that needed to be completed were preprocessing, feature extraction, and classification. There were two kinds of features extracted, namely color feature and texture feature. Experiments were carried out using a variety of different approaches to machine learning. The dataset was differentiated as training and testing data using cross-validation with a k-fold value of 10. The highest results were achieved using the combination of color and texture features with the implementation of K-Nearest Neighbor (KNN) methods. The performance of the method was indicated by the parameters of precision, recall, and accuracy achieved at 92%, 92%, and 92.2%, respectively.

Keywords – cross validation, feature extraction, GLCM, KNN, pre-processing

I. Introduction

Indonesia is a country rich in cultural heritage. The culture is diverse, including dances, ethnicity, race, language, and traditional crafts (*e.g.,* woven, wood carved, traditional batik, and beads). Beads are small decorative objects of various sizes made of stone, bone, shell, glass, plastic, wood, or pearl, with small holes for threading or threading. They are a high-demand product in Indonesia, Malaysia, Europe, and several countries in America.

Nowadays, the fashion of using beads for a variety of purposes continues. The inhabitants of Indonesia's archipelago are familiar with these beads, used as jewelry and as accessories for spiritual or traditional ceremonies. The similarities between the natural environment and the historical and cultural backgrounds of the Indonesian people can be noticed in the bead crafts they create. East Kalimantan's cultural development cannot be divorced from Kalimantan and Indonesian national cultures. Similarly, the origin of beaded products is inextricably linked to other regions.

Beads have evolved in East Kalimantan since their ancestors' time. This is demonstrated by the numerous finds and relics that have come to light in the modern era. Dayak beads are one of the most well-known civilizations. Whereas, the Dayak tribe's beads are distinguished by a range of red, blue, yellow, green, and white hues, each of which has a number of symbolic connotations. The red color signifies the spirit of life, the blue color represents the source of power, the yellow color represents grandeur, the green color represents the universe's wholeness, and the white color represents the sanctity of faith in the creator.

Meanwhile, the use of amethyst indicates an antidote to disease or poison originating in an animal. The Dayak tribe uses many beads to design accessories, such as head coverings, bags, and necklaces, that are worn with their traditional clothing. The lack of

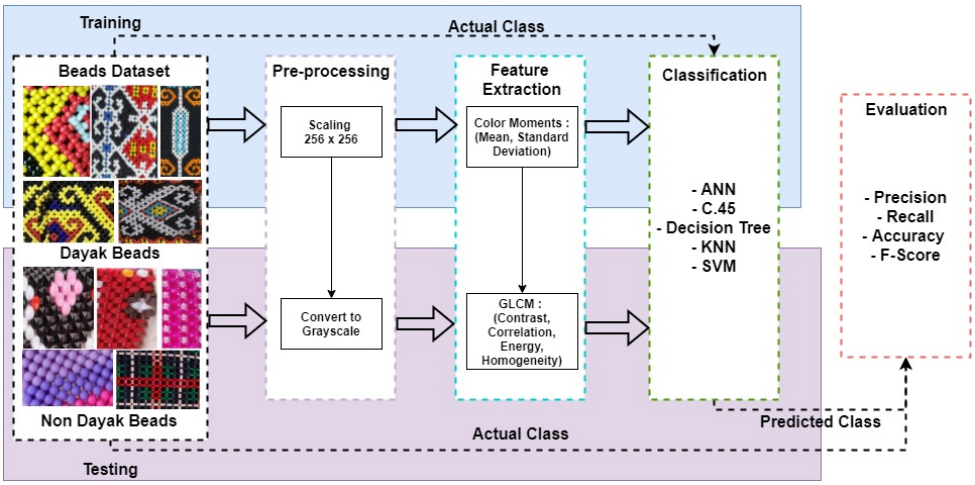

Fig. 1. The primary processes in the proposed method for detecting Dayak beads

automated data collection, the inability to distinguish the beads themselves, which are only owned by select groups, particularly artists, and the wide diversity of bead themes associated with the Dayak tribe make it challenging to identify.

There was no study on traditional crafts related to beads using image data. In recent years, research related to culture that has attracted researchers' interest includes discussing text [1], traditional textile [2], [3], and historical document [4]. Those studies performed image processing techniques requiring three main processes: pre-processing, feature extraction, and classification. In pre-processing, general processes were performed such as image resizing [5] and grayscaling [6], [7]. Subsequently, feature extraction was applied based on color, shape, or texture. Color features were generated using color histogram [8], [9]. While the shape features used, such as statistical features [10], [11]. Commonly used texture features include Local Binary Pattern [12]–[14] and GLCM [6], [15], [16]. Furthermore, classification frequently applied using the method of KNN [12], [17], ANN [18], [19], SVM [20], [21], and Naïve Bayes [22], [23].

The study on the pattern recognition of traditional motifs (Samarinda sarong) was carried out using texture features extracted by the method of color moments, GLCM, and Local Binary Pattern (LBP) and ANN classifier. The dataset consisted of 1000 images, divided into sub-images for learning and testing using cross-validation. The experimental results showed that the average accuracy of the method reaches the maximum value of 100% [7]. Meanwhile, batik and non-batik fabrics were detected in several stages: pre-processing with grayscale technique, texture feature extraction using GLCM, and motif detection using ANN. The dataset used was divided into 70% training data and 30% test data. The ANN model used in this study was a backpropagation learning algorithm with scaled conjugate gradient (trainscg) training and the Lavenberg-Marquardt training method (trainlm). The results obtained for the accuracy with the scaled conjugate gradient (trainscg) algorithm training method was higher, with an accuracy value of 84.12%, compared to the Lavenberg Marquardt algorithm method (trainlm) of 86.11% [19]. Furthermore, the typical Samarinda sarong motif was identified by comparing the color moments, GLCM texture, and CFS feature selection classified using the SVM method. The resulting accuracy achieved 100% by implementing feature selection [24].

This study proposes a method for distinguishing between Dayak and non-Dayak beads. The dataset contains a collection of Dayak and non-Dayak bead images. The color and texture features were extracted using the color moments and GLCM methods. Color features were collected from each RGB color channel. Subsequently, those features were fed through several classifiers, including ANN, C.45, Decision Tree, KNN, and SVM, to demonstrate the most suited method and hence the best performance. Cross-validation was used to apply the classification with a k-fold value of 10.

For a better understanding, the rest of this paper is organized as follows. In section II, we provide the research method, followed by the result in section III. Section IV presents the discussion of the result. Finally, we provide the conclusion in section V.

II. Research Method

The proposed method detected the beads of Dayak and non-Dayak based on the color and texture features using the image processing technique. This method consisted of three primary processes: pre-processing, feature extraction, and classification. An overview of the primary processes sequence for the Dayak bead detection method is depicted in Fig. 1.

A. Dataset

The dataset was formed through the image acquisition process using several tools: a studio minibox with 1 LED lamp and a distance of ± 20 cm, an iPhone

Fig. 2. The example images of the Dayak beads.

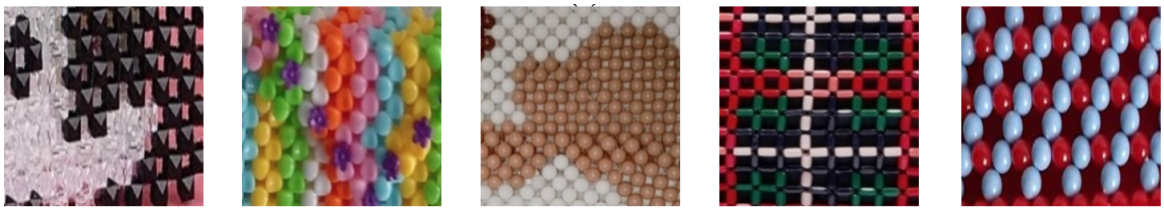

Fig. 3. The example images of the non-Dayak beads.

6s smartphone camera with a resolution of 16 Mega Pixels, and a tripod. The studio minibox used has the size of 15 cm, length 20 cm, and width 23 cm. The beads are placed in the center of the studio minibox with a white background color. The camera position is on a tripod and has a ± 10 cm distance with the beads. The acquired bead image data consists of two types, namely Dayak and non-Dayak. The size of the resulting images was 2000 × 2000 pixels saved in JPEG format. The total number of acquired images was 213 images consisting of 119 images of Dayak beads and 94 images of non-Dayak beads. The example of the acquisition images of Dayak and non-Dayak beads are shown in Fig. 2 and Fig. 3, respectively.

B. Pre-processing

The original image with a resolution of 2000 × 2000 pixels is used as the pre-processing input. The aim of this process is to produce an adequate image; as a result, the results of the following step were optimal in terms of quality. As shown in this study, pre-processing begins with the reduction of the original image's size to 256 × 256 pixels, followed by converting the resizing image into a grayscale image.

C. Feature Extraction

In this study, there were 22 features extracted, which derived from two types of features, namely color, and texture. The color features produced the features of the mean (μ) and standard deviation (σ). These features are extracted in the RGB color space on each channel, including channels R, G, and B. Therefore, there are six color features generated. The value of each color feature is produced using (1) and (2) [9]:

$$\mu = \frac{1}{M \times N} \sum_{i=1}^{M} \sum_{j=1}^{N} X_{ij} \tag{1}$$

$$\sigma = \sqrt{\frac{1}{M \times N} \sum_{i=1}^{M} \sum_{j=1}^{N} \left(X_{ij} - \overline{X_i}\right)^2} \tag{2}$$

M and N are the image sizes, X_{ij} is the pixel value in column i and row j, and X is the average value. Meanwhile, the texture features applied in this study used the Gray Level Co-occurrence Matrix (GLCM) [25] method with several types such as contrast, correlation, energy, and homogeneity with each angle distance. Covering 0°, 45°, 90°, and 135°, the number of texture features produced consists of 16 features. The GLCM was made to quantify the heterogeneity of surface patterns and roughness displayed on digital images [26]. The explanation of each type of GLCM and the equations used are as follows [27]:

1) Contrast (A1) quantifies the presence of the gray level value in the image area. There is a difference in the image's color level or grayscale. If all surrounding pixels have the same value, the contrast value is equal to 0. Eq. (3) is used to calculate the contrast feature, where i is a matrix row, j is matrix column, $P(i, j)$ is an element of the row co-occurrence matrix (i) dan column (j).

$$\sigma = \sqrt{\frac{1}{M \times N} \sum_{i=1}^{M} \sum_{j=1}^{N} \left(X_{ij} - \overline{X_i}\right)^2} \tag{3}$$

with i is a matrix row, j as matrix colum, $P(i, j)$ is an element of the row co-occurrence matrix (i) dan column (j).

2) Correlation (A2) measures the degree of gray level linear dependence in an image, which can be used to visualize the image's linear structure for each pixel adjacent to the image object. The correlation coefficient is between -1 and 1. Eqs. (4), (5), (6), (7), and (8) are used to calculate the correlation feature:

$$A2 = \sum_{i,j} \frac{(i - \mu i)(i - \mu j) P(i, j)}{\sigma_i \sigma_j} \tag{4}$$

$$\mu i = \sum_{i} \sum_{j} i p_{i,j} \tag{5}$$

$$\mu j = \sum_{i} \sum_{j} j p_{i,j} \tag{6}$$

$$\sigma_i = \sqrt{\sum_i \sum_j (i - \mu i)^2 p(i,j)} \quad (7)$$

$$\sigma_j = \sqrt{\sum_i \sum_j (i - \mu i)^2 p(i,j)} \quad (8)$$

where i is the row of the matrix j is the matrix column. $P(i,j)$ is the element of the row (i) and column (j) co-occurrence matrix, (j), μi, μj is the average of the elements in the rows and columns of the matrix, σ_i, σ_j are the standard deviations on the rows and columns of the matrix.

3) Energy (A3) measures the irregularity of the gray level in the image. The value is high if the GLCM elements have relatively the same value. Low value if the GLCM elements are 0 or 1. The energy feature calculation computes using (9), where i is a matrix row, j is a matrix column, $P(i,j)$ is an element of the row co-occurrence matrix (i), and column (j).

$$A3 = \sum_{i,j} P(i,j)^2 \quad (9)$$

4) Homogenity (A4) quantifies the image's homogeneity (similarity). If all pixels have the same value, the homogeneity value will be high. These features are specified in (10), where i is a matrix row, j is a matrix column, $P(i,j)$ is an element of the row co-occurrence matrix (i) and column (j).

$$A4 = \sum_{i_1} \sum_{i_2} \frac{P(i_1, i_2)}{1 + |i_1 - i_2|} \quad (10)$$

D. Classification

In this study, the classification process employs a machine learning approach. Machine learning, a subfield of artificial intelligence, designs and develops algorithms that enable computers to generate behavior in response to empirical data, such as sensor data databases [28]. The application of machine learning in this study was carried out using cross-validation to divide the dataset into two sets: training and testing data. Five classification methods were implemented, including ANN, C.45, Decision Tree, KNN, and SVM as in the previous study [29].

E. Performance Evaluation

The performance of the Dayak beads detection method was evaluated using four parameters: precision, recall, accuracy, and Fscore. Those evaluation parameters are obtained using (11), (12), and (13) [24].

$$precision = \frac{TP}{TP + FP} \times 100 \quad (11)$$

$$recall = \frac{TP}{TP + FN} \times 100 \quad (12)$$

$$accuracy = \frac{TP + TN}{TP + TN + FP + FN} \times 100 \quad (13)$$

True positive (TP) and True negative (TN) are the number of test data classified correctly (target class equal to output class) as Dayak beads class and non-Dayak beads class, respectively. False-positive (FP) is the number of test data of non-Dayak beads class misclassified as Dayak beads class. Meanwhile, False negative (FN) is the number of test data of Dayak beads class misclassified as non-Dayak beads class. The number of TP, TN, FP, and FN is obtained based on the confusion matrix depicted in Fig. 4. The dataset of Dayak beads was subdivided into k sets. In general, training data (k-1)/k were used, while testing data 1/k were used. Subsequently, the procedure was repeated k times. As the last point, the validation result of mean k-time was used as the final rate estimation. The study's performance was determined using 10-fold cross-validation.

		Output Class	
		Dayak beads	***Non-Dayak beads***
Target Class	***Dayak beads***	***TP***	***FN***
	Non-Dayak beads	***FP***	***TN***

Fig. 4. Confusion matrix of Dayak beads detection.

III. RESULT

This section shows the results of each step applied to the proposed method. The processes carried out were pre-processing, feature extraction, classification and method evaluation. The results of each step of the process are described as follows.

Fig. 5. The resulting images of resizing pre-processed.

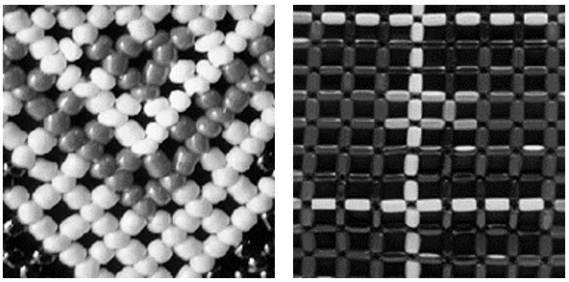

Fig. 6. The resulting images of grayscaling pre-processed.

Table 1. The Extraction Result Example of Color and Texture Features

Image	Color Features	Texture Features
	• μR: 0.706 σR: 0.297 • μG: 0.480 σG: 0.345 • μB: 0.188 σB: 0.182	• $A1_0$: 0.707 $A2_0$: 0.942 $A3_0$: 0.084 $A4_0$: 0.990 • $A1_{45}$: 0.898 $A2_{45}$: 0.927 $A3_{45}$: 0.076 $A4_{45}$: 0.987 • $A1_{90}$: 0.575 $A2_{90}$: 0.953 $A3_{90}$: 0.859 $A4_{90}$: 0.991 • $A1_{135}$: 1.339 $A2_{135}$: 0.908 $A3_{135}$: 0.074 $A4_{135}$: 0.984
	• μR: 0.444 σR: 0.384 • μG: 0.435 σG: 0.370 • μB: 0.162 σB: 0.201	• $A1_0$: 1.324 $A2_0$: 0.899 $A3_0$: 0.059 $A4_0$: 0.981 • $A1_{45}$: 1.856 $A2_{45}$: 0.858 $A3_{45}$: 0.053 $A4_{45}$: 0.976 • $A1_{90}$: 0.932 $A2_{90}$: 0.928 $A3_{90}$: 0.064 $A4_{90}$: 0.064 • $A1_{135}$: 1.916 $A2_{135}$: 0.854 $A3_{135}$: 0.053 $A4_{135}$: 0.053
	• μR: 0.309 σR: 0.329 • μG: 0.287 σG: 0.304 • μB: 0.158 σB: 0.240	• $A1_0$: 2.045 $A2_0$: 0.844 $A3_0$: 0.105 $A4_0$: 0.972 • $A1_{45}$: 2.379 $A2_{45}$: 0.819 $A3_{45}$: 0.102 $A4_{45}$: 0.969 • $A1_{90}$: 1.134 $A2_{90}$: 0.931 $A3_{90}$: 0.121 $A4_{90}$: 0.983 • $A1_{135}$: 2.569 $A2_{135}$: 0.804 $A3_{135}$: 0.100 $A4_{135}$: 0.967
	• μR: 0.428 σR: 0.366 • μG: 0.413 σG: 0.378 • μB: 0.420 σB: 0.386	• $A1_0$: 0.357 $A2_0$: 0.890 $A3_0$: 0.122 $A4_0$: 0.994 • $A1_{45}$: 0.499 $A2_{45}$: 0.846 $A3_{45}$: 0.107 $A4_{45}$: 0.992 • $A1_{90}$: 0.347 $A2_{90}$: 0.893 $A3_{90}$: 0.124 $A4_{90}$: 0.994 • $A1_{135}$: 0.490 $A2_{135}$: 0.848 $A3_{135}$: 0.106 $A4_{135}$: 0.992
	• μR: 0.410 σR: 0.466 • μG: 0.415 σG: 0.368 • μB: 0.404 σB: 0.487	• $A1_0$: 0.348 $A2_0$: 0.754 $A3_0$: 0.123 $A4_0$: 0.991 • $A1_{45}$: 0.421 $A2_{45}$: 0.653 $A3_{45}$: 0.114 $A4_{45}$: 0.993 • $A1_{90}$: 0.317 $A2_{90}$: 0.651 $A3_{90}$: 0.112 $A4_{90}$: 0.998 • $A1_{135}$: 0.414 $A2_{135}$: 0.852 $A3_{135}$: 0.117 $A4_{135}$: 0.991
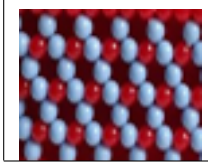	• μR: 0.345 σR: 0.378 • μG: 0.423 σG: 0.352 • μB: 0.421 σB: 0.412	• $A1_0$: 0.342 $A2_0$: 0.780 $A3_0$: 0.112 $A4_0$: 0.978 • $A1_{45}$: 0.415 $A2_{45}$: 0.568 $A3_{45}$: 0.117 $A4_{45}$: 0.932 • $A1_{90}$: 0.364 $A2_{90}$: 0.421 $A3_{90}$: 0.321 $A4_{90}$: 0.914 • $A1_{135}$: 0.123 $A2_{135}$: 0.842 $A3_{135}$: 0.116 $A4_{135}$: 0.929

In the pre-processing, applied image resizing and conversion from RGB image to grayscale. The application of resizing images is needed to speed up the computational process by reducing the pixel size of the image. The original sarong image data, 2000 × 2000 pixels, was applied to a resize operation to 256 × 256 pixels. Furthermore, the resized image was converted into a grayscale image to simplify the texture feature extraction process calculations. The resulting images of pre-processing are depicted in Fig. 5 and Fig. 6.

In feature extraction, 22 feature values were generated from each sarong image. The feature used is color with Color Moments consisting of the mean (μ) and standard deviation (σ) generated from each RGB color channel. Meanwhile, the texture features are generated using the GLCM method, which includes features of contrast (F1), correlation (F2), energy (F3), and homogeneity (F4) with angles of 0°, 45°, 90°, and 135°, respectively. The examples values of feature extraction results from Dayak and non-Dayak beads are presented in Table 1.

IV. Discussion

The proposed method had the best accuracy for some features. Therefore, several experiments were carried out to justify the appropriate method against the dataset used in this study. The method evaluation was carried out using several feature sets extracted at color and texture features, fed into five classifiers, including ANN, C.45 Decision Tree, Decision Tree, KNN, and SVM. The Dayak bead identification method test was developed using 330 images divided into 206 Dayak beads and 124 non-Dayak beads. The classifiers were implemented using cross-validation with the value of k-fold 10. The experiments were carried out using different types of features, including color, texture, and overall features. The method performance of Dayak beads detection was evaluated using four parameters: precision (P), recall (R), and accuracy (A). The experiment results using different features and classifiers are summarized in Table 2.

Table 2 shows the use of color and texture features separately; also, a combination of both features affects the proposed method's performance. In this study, the highest value of accuracy and F-score were

Table 2. The Experiment Results using Different Features and Classifiers

Classifier	Color + Texture (%)			Color (%)			Texture (%)		
	P	R	A	P	R	A	P	R	A
ANN	89.7	89.7	89.7	89.7	89.7	89.7	81.7	81.7	81.7
C.45	86.9	86.9	86.9	86.2	85.9	85.9	79.3	79.3	79.3
Decision Tree	85.0	85.0	84.9	87.8	87.8	87.8	69.4	69.5	69.5
KNN	92.0	92.0	92.2	89.7	89.7	89.7	73.3	73.2	73.3
SVM	89.1	88.7	88.7	86.8	86.9	86.9	81.7	81.7	81.7

achieved at 92.2% and 92%, respectively. These results were obtained using the incorporation of color and texture features with the KNN classifier. Otherwise, Table 2 shows the decision tree classifier obtained the lowest accuracy value of 69.5% based on the texture features. Table 2 indicates the color features are more discriminating than texture features, but the use of both features can improve the proposed method's performance. Furthermore, details of the number of testing data classified correctly and the misclassification that occurred presented by the confusion matrix are depicted in Fig. 7, Fig. 8, and Fig. 9.

Based on Fig. 7, Fig. 8, and Fig. 9, the detection fallacy often occurs in the non-Dayak beads class that was detected as the Dayak beads class. It happens visually that non-Dayak beads tend to have a similar color and texture to the Dayak beads pattern. Based on the classification results presented in Fig. 7, Fig. 8, and Fig. 9, the combination features of color and texture can reduce the number of misclassifications.

V. Conclusion

Various types of beads are made by different ethnicities in Indonesia, such as the Dayak beads. This study developed a machine-learning approach to detect beads to distinguish between Dayak and non-Dayak based on color and texture features. The method input was beads images and consisted of three main processes: pre-processing, feature extraction, and classification. Pre-processing was applied to resize the image and converting to a grayscale image. Both were applied to reduce the computational time and simplify the subsequent process. The features used are 22, obtained from six color features and 16 texture features. The color features were extracted based on each channel's mean and standard deviation in RGB color space. In contrast, the texture features were generated using the GLCM method by computing the value of the contrast, correlation, energy, and homogeneity. The classification was implemented using cross-validation with the k-fold value of 10 with the KNN classifier. The performance of the proposed method achieved the value of precision, recall, and accuracy were 92%, 92%, and 92%, respectively. The detection method of beads types or similar objects can still be developed widely using various techniques to overcome the misclassification in this study.

Acknowledgement

This research was supported by the Faculty of Engineering, Mulawarman University, and Faculty of Information Technology & Industry, Universitas Stikubank.

References

[1] M. P. Singh and G. Singh, "Two phase learning technique in modular neural network for pattern classification of handwritten Hindi alphabets," *Mach. Learn. with Appl.*, vol. 6, no. December, pp. 100174, 2021.

[2] A. Ramadhanu, J. Na'am, G. W. Nurcahyo, and Yuhandri, "Development of affine transformation method in the reconstruction of songket motif," *Int. J. Adv. Sci. Eng. Inf. Technol.*, vol. 12, no. 2, pp. 600–606, 2022.

[3] T. Hu, Q. Xie, Q. Yuan, J. Lv, and Q. Xiong, "Design of ethnic patterns based on shape grammar and artificial neural network", *Alexandria Eng. J.*, vol. 60, No. 1, pp. 1601–1625, 2021.

[4] S. Zhalehpour, E. Arabnejad, C. Wellmon, A. Piper, and M. Cheriet, "Visual information retrieval from historical document images," *J. Cult. Herit.*, vol. 40, pp. 99–112, 2019.

[5] R. Andrian, B. Hermanto, and R. Kamil, "The implementation of backpropagation artificial neural network for recognition of batik Lampung motive," *J. Phys. Conf. Ser.*, vol. 1338, no. 1, 2019.

[6] C. I. Ossai and N. Wickramasinghe, "GLCM and statistical features extraction technique with extra-tree classifier in macular oedema risk diagnosis," *Biomed. Signal Process. Control*, vol. 73, no. March, pp. 103471, 2022.

[7] A. Septiarini, R. Saputra, A. Tejawati, M. Wati, and H. Hamdani, "Pattern recognition of sarong fabric using machine learning approach based on computer vision for cultural preservation," *Int. J. of Intelligent Engineering and Systems*, vol. 15, no. 5, pp. 284–295, 2022.

[8] H. Hamdani, A. Septiarini, A. Sunyoto, S. Suyanto, and F. Utaminingrum, "Detection of oil palm leaf disease based on color histogram and supervised classifier," *Opt. - Int. J. Light Electron Opt.*, vol. 245, no. 167753, pp. 2–5, 2021.

[9] S. Ramesh and D. Vydeki, "Recognition and classification of paddy leaf diseases using optimized deep neural network with jaya algorithm," *Inf. Process. Agric.*, vol. 7, no. 2, pp. 249–260, 2020.

[10] Farida, R. E. Caraka, T. W. Cenggoro, and B. Pardamean, "Batik parang rusak detection using geometric invariant moment," in *1st 2018 Indones. Assoc. Pattern Recognit. Int. Conf. Ina. 2018 - Proc.*, pp. 71–74, 2019.

[11] T. Hu, Q. Xie, Q. Yuan, J. Lv, and Q. Xiong, "Design of ethnic patterns based on shape grammar and artificial neural network," *Alexandria Eng. J.*, vol. 60, no. 1, pp. 1601–1625, 2021.

[12] A. H. Rangkuti, A. Harjoko, and A. Putra, "A novel reliable approach for image batik classification that invariant with scale and rotation using MU2ECS-LBP algorithm," *Procedia Comput. Sci.*, vol. 179, no. 2019, pp. 863–870, 2021.

[13] X. Shu, Z. Song, J. Shi, S. Huang, and X. Wu, "Multiple channels local binary pattern for color texture representation and classification," *Signal Processing: Image Communication*, vol. 98, pp. 116392, 2021.

[14] J. Rajevenceltha and V. H. Gaidhane, "An efficient approach for no-reference image quality assessment based on statistical texture and structural features," *Eng. Sci. Technol. an Int. J.*, In Press, 2021.

[15] M. J. Pendekal and S. Gupta, "An ensemble classifier based on individual features for detecting microaneurysms in diabetic retinopathy," *Indonesian Journal of Electrical Engineering and Informatics*, vol. 10, no. 1, pp. 60–71, 2022.

[16] Y. Jusman, N. S. Cheok, and K. Hasikin, "Performances of proposed normalization algorithm for iris recognition," *Int. J. Adv. Intell. Informatics*, vol. 6, no. 2, pp. 161-172, 2020.

[17] N. Setiyawati, "A proposed classification method in menu engineering using the k-nearest neighbors algorithm," *Int. J. Adv. Sci. Eng. Inf. Technol.*, vol. 11, no. 4, pp. 1360–1365, 2021.

[18] A. Septiarini, A. Sunyoto, H. Hamdani, A. Ahmad, F. Utaminingrum, and H. Rahmania, "Machine vision for the maturity classification of oil palm fresh fruit bunches based on color and texture features," *Sci. Hortic.*, vol. 286, no. 110245, pp. 1–15, 2021.

[19] A. Kasim, M. Bakri, and A. Septiarini, "The artificial neural networks (ANN) for batik detection based on textural features," *Proceedings of the 7th Mathematics, Science, and Computer Science Education International Seminar, MSCEIS*, 2019.

[20] K. R. Singh, K.P. Neethu, K. Madhurekaa, A. Harita, and P. Mohan, "Parallel SVM model for forest fire prediction," *Soft Computing Letters*, vol. 3, no. December, pp. 100014, 2021.

[21] M. Ameliasari, A. G. Putrada, and R. R. Pahlevi, "An evaluation of SVM in hand gesture detection using IMU-based smartwatches for smart lighting control," *Jurnal Infotel*, vol. 13, no. 2, pp. 47–53, 2021.

[22] I. K. A. Enriko, M. Melinda, A. C. Sulyani, and I. G. B. Astawa, "Breast cancer recurrence prediction system using k- nearest neighbor, naïve-bayes, and support vector machine algorithm," *Jurnal Infotel*, vol. 13, no. 4, pp. 185–188, 2021.

[23] C. E. Chandra and S. Abdullah, "Forecasting mortality trend of Indonesian old aged population with bayesian method," *Int. J. Adv. Sci. Eng. Inf. Technol.*, vol. 12, no. 2, pp. 580–606588, 2022.

[24] A. Septiarini, R. Saputra, M. Wati, H. Hamdani, A. Tejawati, and N. Puspitasari, "Analysis of color and texture features for Samarinda sarong classification," in *4th International Seminar on Research of Information Technology and Intelligent Systems (ISRITI) 2021*, pp. 1–6, 2021.

[25] N. M. Saad, A. R. Abdullah, W. H. W. Hasan, N. N. S. A. Rahman, N. H. Ali, and I. N. Abdullah, "Automated vision based defect detection using gray level co-occurrence matrix for beverage manufacturing industry," *IAES Int. J. Artif. Intell.*, vol. 10, no. 4, pp. 818–829, 2021.

[26] Z. Rustam, A. Purwanto, S. Hartini, and G. S. Saragih, "Lung cancer classification using fuzzy C-means and fuzzy Kernel C-means based on CT scan image," *IAES Int. J. Artif. Intell.*, vol. 10, no. 2, pp. 291–297, 2021.

[27] F. Utaminingrum, A. W. Satria Bahari Johan, K. Somawirata, Risnandar, and A. Septiarini, "Descending stairs and floors classification as control reference in autonomous smart wheelchair," *J. King Saud Univ. - Comput. Inf. Sci.*, no. 34, pp. 6040–6047, 2022.

[28] A. Kececi, A. Yildirak, K. Ozyazici, G. Ayluctarhan, O. Agbulut, and I. Zincir, "Implementation of machine learning algorithms for gait recognition," *Eng. Sci. Technol. an Int. J.*, vol. 23, no. 4, pp. 931–937, 2020.

[29] R. S. El-Sayed and M. N. El-Sayed, "Classification of vehicles' types using histogram oriented gradients: Comparative study and modification," *IAES Int. J. Artif. Intell.*, vol. 9, no. 4, pp. 700–712, 2020.

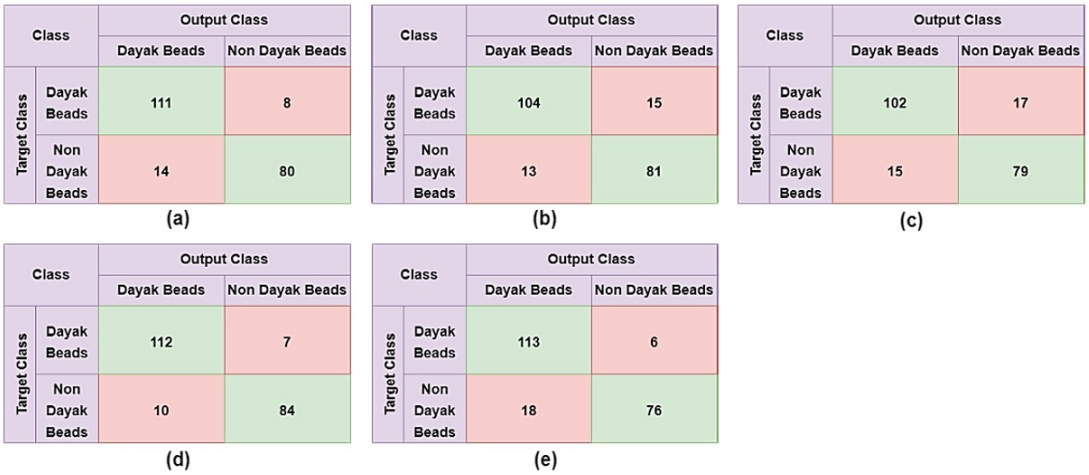

Fig. 7. Confusion matrix based on color and texture features using: (a) ANN, (b) C.45, (c) SVM, (d) Decision Tree, and (e) KNN.

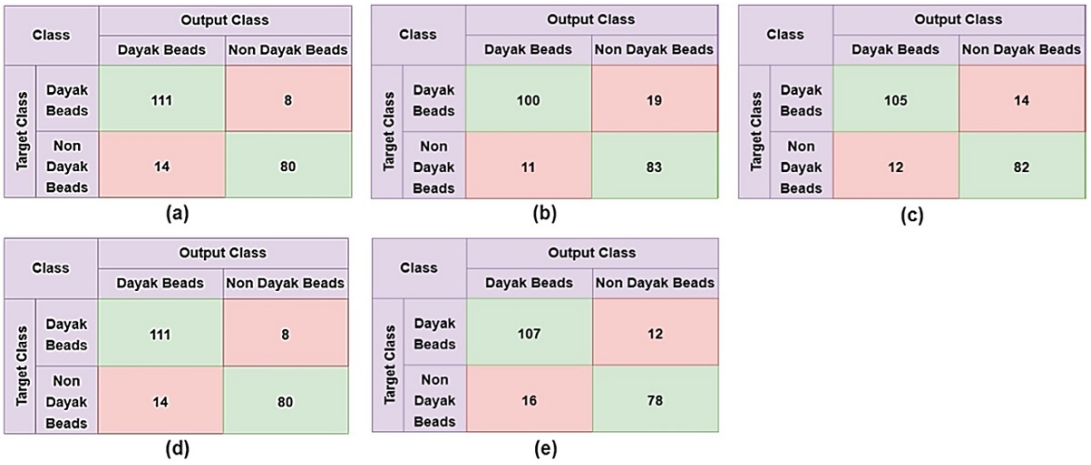

Fig. 8. Confusion matrix based on color features using: (a) ANN, (b) C.45, (c) Decision Tree, (d) KNN, and (e) SVM.

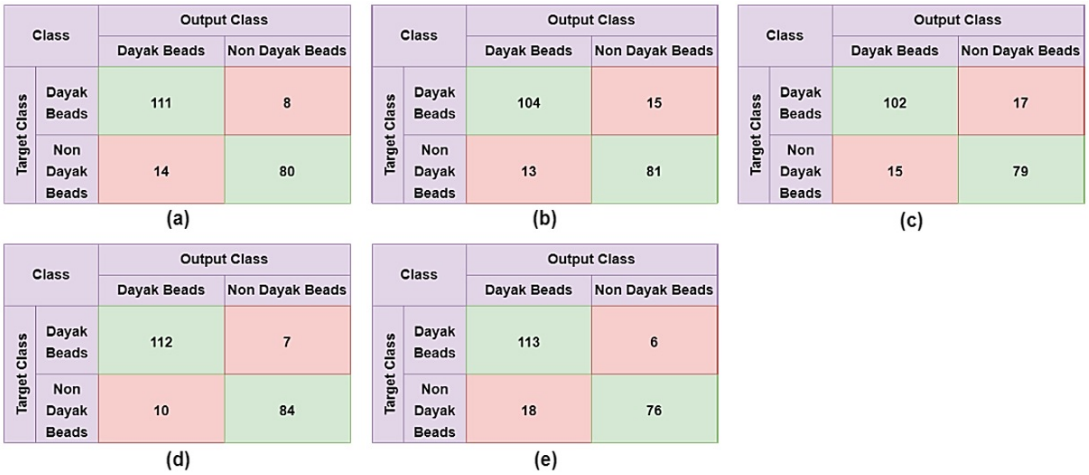

Fig. 9. Confusion matrix based on texture features using: (a) ANN, (b) C.45, (c) Decision Tree, (d) KNN, and (e) SVM.